EMBO reports

scientific report

# Mammalian Ku86 protein prevents telomeric fusions independently of the length of TTAGGG repeats and the G-strand overhang

Enrique Samper[1], Fermín A. Goytisolo[1], Predrag Slijepcevic[2], Paul P.W. van Buul[3] and María A. Blasco[1,+]

[1]Department of Immunology and Oncology, Centro Nacional de Biotecnología, Spain, [2]Department of Biological Sciences, Brunel University, UK and [3]Department of Radiation Genetics and Chemical Mutagenesis, Leiden University, The Netherlands

Received June 8, 2000; revised June 30, 2000; accepted July 25, 2000

**Ku86 together with Ku70, DNA-PKcs, XRCC4 and DNA ligase IV forms a complex involved in repairing DNA double-strand breaks (DSB) in mammals. Yeast Ku has an essential role at the telomere; in particular, Ku deficiency leads to telomere shortening, loss of telomere clustering, loss of telomeric silencing and deregulation of the telomeric G-overhang. In mammals, Ku proteins associate to telomeric repeats; however, the possible role of Ku in regulating telomere length has not yet been addressed. We have measured telomere length in different cell types from wild-type and Ku86-deficient mice. In contrast to yeast, Ku86 deficiency does not result in telomere shortening or deregulation of the G-strand overhang. Interestingly, Ku86$^{-/-}$ cells show telomeric fusions with long telomeres (>81 kb) at the fusion point. These results indicate that mammalian Ku86 plays a fundamental role at the telomere by preventing telomeric fusions independently of the length of TTAGGG repeats and the integrity of the G-strand overhang.**

## INTRODUCTION

Double-strand breaks (DSB) are generated by reactive by-products of the oxygen metabolism, exposure to ionizing radiation and in V(D)J recombination in lymphocytes. The mammalian DNA-PK complex is essential for both DNA DSB repair and for V(D)J recombination. In mammals, DNA-PK is composed of a catalytic subunit, DNA-PKcs and a regulatory factor, Ku, which is a heterodimer of two proteins, Ku70 and Ku86. In yeast there is no DNA-PKcs subunit. Yeast Ku heterodimer binds with high affinity to DNA ends (Smith and Jackson, 1999). Mutant yeast Ku86 results in defective DSB repair (Boulton and Jackson, 1996). Similarly, mice deficient for Ku70, Ku86 or DNA-PKcs show defective DSB repair and V(D)J recombination, and are hypersensitive to ionizing radiation (Blunt *et al.*, 1996; Nussenzweig *et al.*, 1996; Zhu *et al.*, 1996; Gu *et al.*, 1997; Ouyang *et al.*, 1997; Gao *et al.*, 1998), suggesting a similar role of Ku proteins in DSB repair in mammals.

Telomeres are the ends of eukaryotic chromosomes and, in vertebrates, consist of tandem repeats of the sequence TTAGGG (Blackburn, 1991). TTAGGG repeats, together with telomeric proteins, stabilize chromosome ends, preventing end-to-end fusions (Counter *et al.*, 1992; Blasco *et al.*, 1997). Some telomeric proteins, such as TRF2 in mammals, are essential for telomere function independently of telomere length (van Steensel *et al.*, 1998). Telomeric sequences are lost during *in vitro* culture of primary cells and with increasing age in some adult tissues, and impairment of telomere function by loss of telomeric sequences have been shown to limit the proliferative capacity of cultured cells and to affect the organismal life span (Autexier and Greider, 1996). Interestingly, studies in yeast show that Ku has a role at the telomere in addition to the role in non-homologous end joining (NHEJ). In particular, yeast defective in either Ku subunit show a 60% loss of telomeric repeats, loss of telomere clustering, loss of telomeric silencing and deregulation of the G-strand overhang (Boulton and Jackson, 1996, 1998; Gravel *et al.*, 1998; Laroche *et al.*, 1998; Nugent *et al.*, 1998). Furthermore, yeast Ku moves from the telomeres to the DSB upon induction of damage, suggesting a link between DNA repair and the telomeres (Martin *et al.*, 1999; Mills *et al.*, 1999). Mammalian Ku can also bind to telomeric sequences (Bianchi

+Corresponding author. Tel: +34 915 854 846; Fax: +34 913 720 493; E-mail: mblasco@cnb.uam.es

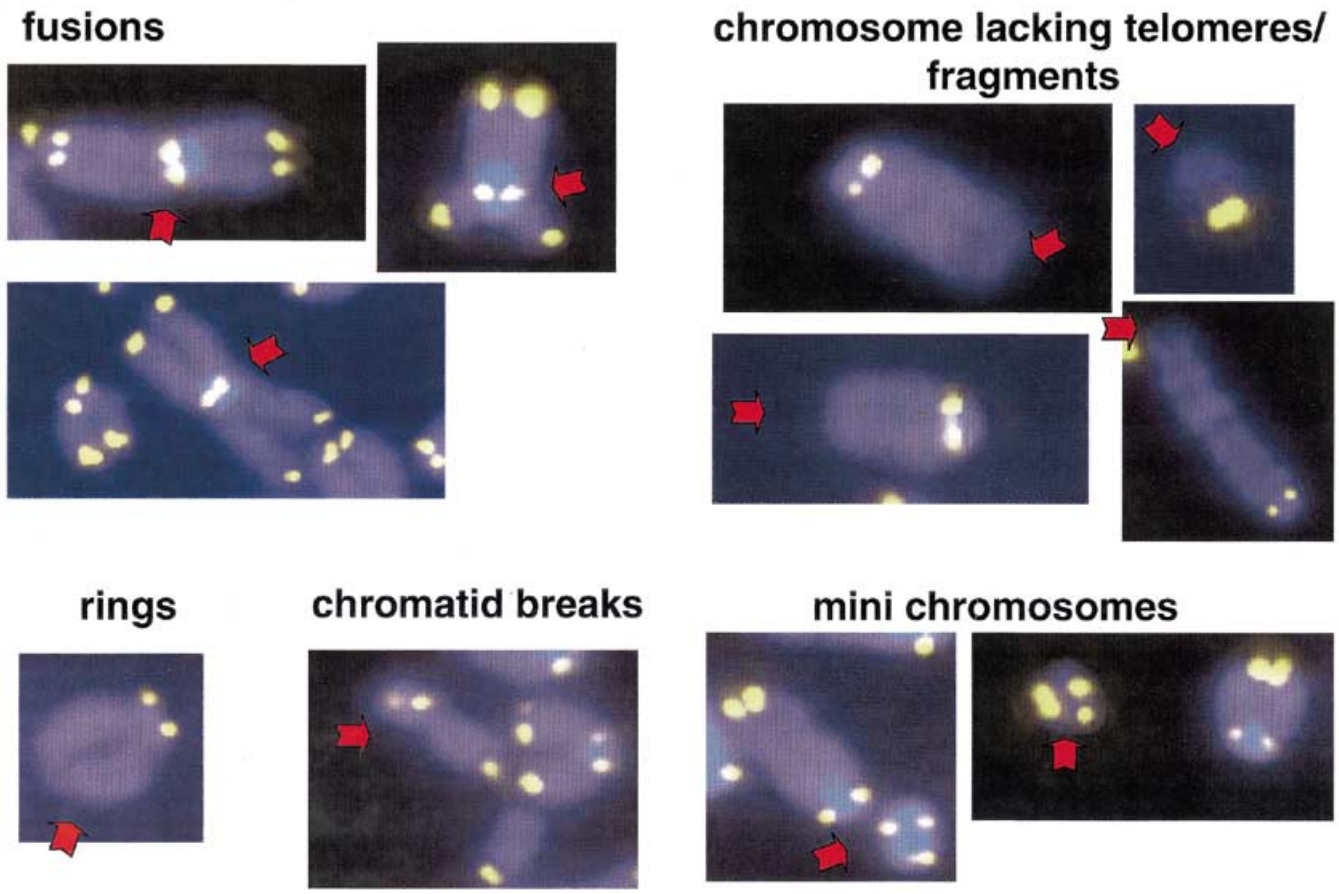


**Fig. 1.** Chromosome aberrations in Ku86$^{-/-}$ primary MEFs. Cytogenetic alterations detected in Ku86$^{-/-}$ metaphases from primary MEFs after hybridization with DAPI and a fluorescent Cy-3 labelled PNA-telomeric probe. For quantifications see Table I. Blue colour corresponds to chromosome DNA stained with DAPI; yellow and white dots correspond to TTAGGG repeats; red arrows highlight each of the different chromosomal abnormalities shown in the figure.

and de Lange, 1999; Hsu *et al.*, 1999) and prevent end-to-end fusions (Bailey *et al.*, 1999).

To determine whether Ku86 deficiency has an effect on telomere length and/or the integrity of the G-strand, we measured telomere length in wild-type and Ku86$^{-/-}$ cells. In contrast to yeast, Ku86 deficiency in mammals results in neither shortening of telomeres nor in loss of the G-strand overhang. We found numerous chromosomal aberrations in Ku86$^{-/-}$ cells, including telomeric fusions. Q-FISH analysis of the telomeric fusions, however, shows that they have long telomeres at the fusion point, indicating that mammalian Ku86 prevents end-to-end fusions independently of the length of TTAGGG repeats.

## RESULTS

### Ku86 protects telomeres from fusions independently of the length of TTAGGG repeats

Previous works showed increased chromosomal instability and telomeric fusions in Ku86 deficient cells (Bailey *et al.*, 1999; Difilippantonio *et al.*, 2000). To address the involvement of telomeres in the chromosomal instability of Ku86$^{-/-}$ cells, we performed quantitative FISH with a fluorescent PNA-telomeric probe (Zijlmans *et al.*, 1997) on metaphases from primary (passage 1) wild-type and Ku86$^{-/-}$ mouse embryonic fibroblasts (MEFs) derived from heterozygous crosses. Our analysis reveals that Ku86$^{-/-}$ cells MEFs show a 24-fold increase in telomeric fusions as compared with wild-type cells, a 6.25-fold increase in broken chromatids, and a 6.6-fold increase in chromosome fragments (Figure 1; Table I). All telomeric fusions contained telomeres at the fusion point of an average length of 81.6 ± 5.3 kb, suggesting that these fusions did not occur due to loss of telomeric sequences. Indeed, a telomere length of 81 kb is consistent with the sum of two wild-type telomeres.

### Ku86 deficiency in mammals does not result in telomere shortening

Ku86$^{-/-}$ deficiency in yeast produces a dramatic telomere shortening (Boulton and Jackson, 1996). To examine this possibility in mammals, littermate wild-type and Ku86$^{-/-}$ mice or embryos derived from heterozygous crosses were used to quantify telomere length. The following cell types were analysed in wild-type and Ku86$^{-/-}$ mice: primary MEFs (passage 1), fresh bone

**Table I.** Cytogenetic analysis of wild-type and Ku86$^{-/-}$ primary MEFs (passage 2) using a PNA-telomeric probe

| Cell type[a] | No. of metaphases | Telomeric fusions | Chromosomes lacking telomeres | Chromosome fragments (0 or 2 telomeres) | Chromatid breaks | Mini-chromosomes (4 telomeres) | Rings |
|---|---|---|---|---|---|---|---|
| Wt (D5) | 56 | 0 | 2 | 6 | 1 | 0 | 0 |
| Ku86$^{-/-}$ (D1) | 65 | 16 | 8 | 34 | 36 | 0 | 7 |
| Wt (A3) | 66 | 1 | 2 | 4 | 5 | 0 | 0 |
| Ku86$^{-/-}$ (A1) | 57 | 0 | 1 | 2 | 4 | 0 | 0 |
| Wt (H4) | 53 | 0 | 0 | 2 | 0 | 0 | 0 |
| Ku86$^{-/-}$ (H6) | 56 | 8 | 4 | 22 | 4 | 2 | 2 |
| Wt (K1) | 56 | 0 | 0 | 4 | 3 | 1 | 0 |
| Ku86$^{-/-}$ (K4) | 56 | 14 | 3 | 27 | 10 | 1 | 8 |
| Wt (K2) | 55 | 1 | 0 | 0 | 1 | 0 | 0 |
| Ku86$^{-/-}$ (K9) | 55 | 14 | 0 | 19 | 8 | 0 | 7 |
| Wt (I6) | 40 | 1 | 0 | 5 | 2 | 0 | 0 |
| Ku86$^{-/-}$ (I2) | 40 | 19 | 0 | 35 | 13 | 0 | 4 |

[a]Wild-type and Ku86$^{-/-}$ embryos that are named with the same letter (ie. D1 and D5) correspond to littermate embryos derived from heterozygous crosses.

**Table II.** Telomere length in wild-type and Ku86$^{-/-}$ cells as determined by Q-FISH

| Genotype cell type[a] | p-arm (kb) | q-arm (kb) | p+q arm (kb) | Metaphase No. |
|---|---|---|---|---|
| WT (D5) MEF | 43.48 ± 0.28 | 55.48 ± 0.48 | 49.48 ± 0.38 | 15 |
| Ku86$^{-/-}$ (D1) MEF | 46.25 ± 0.33 | 66.80 ± 0.054 | 56.52 ± 0.44 | 15 |
| WT (I6) MEF | 41.37 ± 0.28 | 54.00 ± 0.36 | 47.68 ± 0.32 | 15 |
| Ku86$^{-/-}$ (I2) MEF | 42.06 ± 0.29 | 59.95 ± 0.47 | 51.01 ± 0.38 | 15 |
| WT (A3) MEF | 42.79 ± 0.33 | 56.35 ± 0.46 | 49.57 ± 0.40 | 15 |
| Ku86$^{-/-}$ (A1) MEF | 42.93 ± 0.22 | 54.05 ± 0.29 | 48.49 ± 0.25 | 15 |
| WT (H4) MEF | 40.38 ± 0.34 | 48.30 ± 0.36 | 44.34 ± 0.35 | 15 |
| Ku86$^{-/-}$ (H6) MEF | 45.06 ± 0.29 | 57.99 ± 0.42 | 51.52 ± 0.36 | 15 |
| WT (K1) MEF | 37.41 ±.024 | 54.97 ± 0.44 | 46.19 ± 0.34 | 15 |
| Ku86$^{-/-}$ (K4) MEF | 41.49 ± 0.25 | 56.09 ± 0.35 | 48.79 ± 0.30 | 15 |
| WT (K2) MEF | 40.81 ± 0.27 | 52.75 ± 0.32 | 46.78 ± 0.30 | 15 |
| Ku86$^{-/-}$ (K9) MEF | 41.57 ± 0.28 | 57.84 ± 0.42 | 49.71 ± 0.35 | 15 |
| WT (101) BM | 43.98 ± 0.25 | 55.50 ± 0.38 | 49.74 ± 0.32 | 10 |
| Ku86$^{-/-}$ (100) BM | 48.63 ± 0.36 | 68.20 ± 0.54 | 58.41 ± 0.45 | 10 |

[a]Wild-type and Ku86$^{-/-}$ embryos that are named with the same letter (ie. D5 and D1) correspond to littermate embryos coming from heterozygous parents. All cells are MEFs except for 101 and 100, which are bone marrow cultures (BM).

marrow (BM), fresh splenocytes and premeiotic male germ cells. To measure telomere length we used three different quantitative techniques: (i) Q-FISH on metaphases (MEFs, BM, premeiotic male germ cells), (ii) FLOW-FISH on BM cells and splenocytes, and (iii) TRF on both MEFs and BM cells (see Methods). Q-FISH was carried out in two different laboratories: Madrid and Leiden.

## Q-FISH on MEFs, BM cells and premeiotic germ cells

Q-FISH analysis of six littermate pairs of wild-type and Ku86$^{-/-}$ MEFs revealed that Ku86$^{-/-}$ cells had similar or slightly extended telomeres compared with wild type (Table II; Figure 2A). The average telomere length was 51.01 ± 1.2 kb and 47.34 ± 0.82 kb for Ku86$^{-/-}$ and wild-type MEFs, respectively (see Madrid section of Methods). Similarly, Q-FISH analysis of BM spreads showed telomere lengths of 49.74 ± 0.32 kb and 58.41 ± 0.45 kb for wild-type and Ku86$^{-/-}$ littermates, respectively (Table II). The Q-FISH data on MEFs were confirmed by performing FLOW-FISH of the same MEFs (see Madrid section of Methods) (Figure 3A), and the average telomere fluorescence expressed in arbitrary units was 11.56 ± 0.22 and 12.67 ± 0.13 for wild-type and Ku86$^{-/-}$ BM, respectively. Histograms showing the frequency of a given telomere fluorescence in all six wild-type and Ku86$^{-/-}$ MEFs analysed in this study are presented in Figure 3B. These histograms show that the mean telomere fluorescence is similar in Ku86$^{-/-}$ to that in wild-type MEFs; furthermore, the heterogeneity of telomeric lengths is similar in both genotypes.

Telomeric Q-FISH analysis on BM and premeiotic male germ cells (testes) from littermate wild-type and Ku86$^{-/-}$ mice was

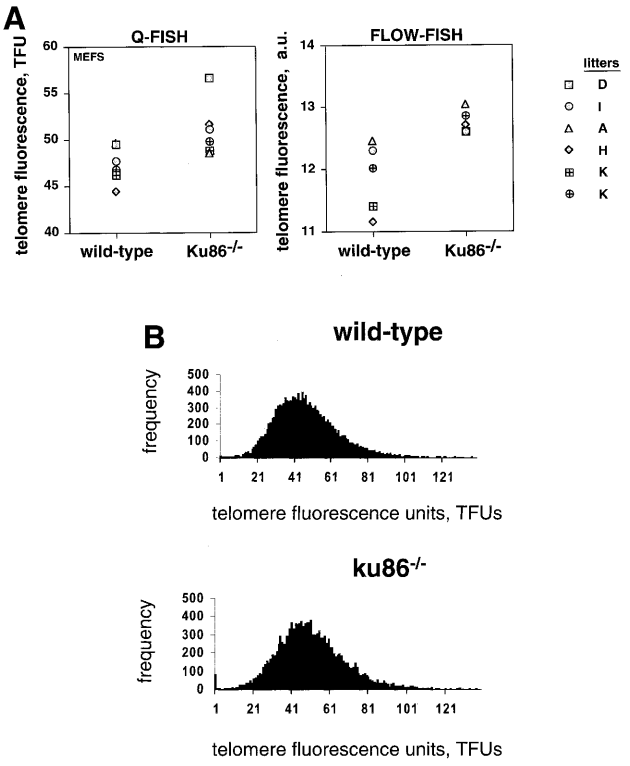


**Fig. 2.** Telomere analysis of littermate wild-type and Ku86$^{-/-}$ MEFs by Q-FISH and FLOW-FISH. (**A**) Telomere fluorescence of littermate wild-type and Ku86$^{-/-}$ MEFs (passage 1) by Q-FISH and FLOW-FISH (Madrid section in Methods). (**B**) Telomere length distribution of at least 14 000 telomeres in six different littermate wild-type and Ku86$^{-/-}$ primary MEFs. The histogram depicts similar telomeres in Ku86$^{-/-}$ and wild-type cells. 1 TFU corresponds to 1 kb of TTAGGG repeats.

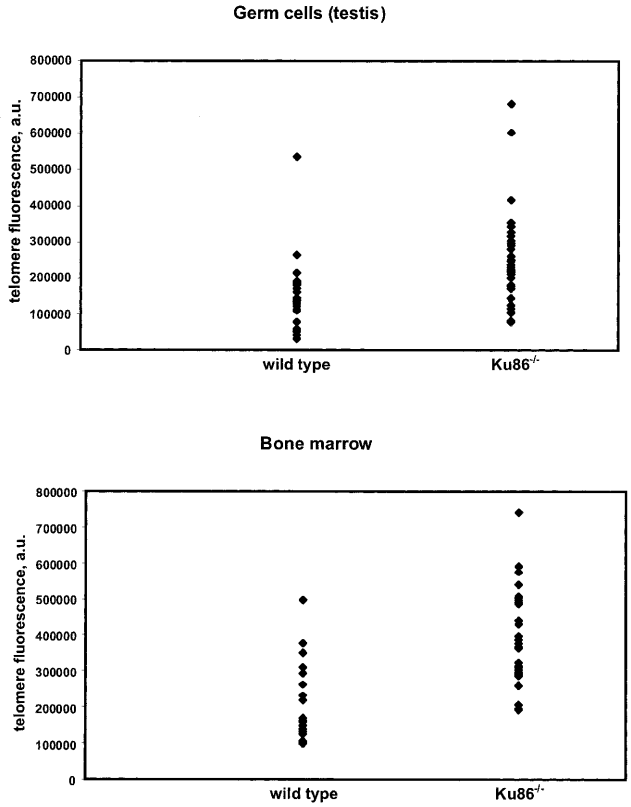


**Fig. 3.** Telomere length analysis of littermate wild-type and Ku86$^{-/-}$ BM and male premeiotic germ cells by Q-FISH. Telomere fluorescence of littermate wild-type and Ku86$^{-/-}$ nuclei by Q-FISH (Leiden section in Methods). Telomere fluorescence of interphase nuclei from two wild-type and Ku86$^{-/-}$ littermates is represented in arbitrary units; each point represents an individual nucleus. Both bone marrow and diploid premeiotic male germ cell nuclei were analysed. BM: wild-type, 28 nuclei; Ku86$^{-/-}$, 35 nuclei. Testis: wild-type, 27 nuclei; Ku86$^{-/-}$ 39 nuclei.

carried out using a different Q-FISH protocol (see Leiden section of Methods). Figure 3 shows telomere fluorescence in BM and sperm cell nuclei from two wild-type and two Ku86$^{-/-}$ littermate mice (8–10 weeks old). In both cell types, telomere fluorescence in Ku86$^{-/-}$ nuclei was similar or higher than in the wild-type controls, in agreement with previous results.

## FLOW-FISH on primary splenocytes and BM cells

FLOW-FISH on fresh wild-type and Ku86$^{-/-}$ splenocytes and BM cells derived from six litters of mice (8–12 weeks old) also indicated that Ku86$^{-/-}$ telomeres were similar or longer than those of wild-type littermates (Table III), in agreement with the Q- and FLOW-FISH data on MEFs.

## TRF analysis of MEF and BM cells

We also used Southern blotting to measure telomere length as a different technique not based on FISH. Primary wild-type and Ku86$^{-/-}$ MEFs and BM cells were subjected to TRF analysis as described (see Methods). As shown in Figure 4, telomere restriction fragments (TRF) were of a similar length in littermate wild-type and Ku86$^{-/-}$ cells.

Together, these data indicate that Ku86$^{-/-}$ deficiency in mammals does not result in telomere shortening as is the case for yeast (Boulton and Jackson, 1996). Indeed, Ku86 deficiency in mammals results in moderately extended telomeres. We were not able to address the possibility of a delayed telomere length phenotype for Ku86 deficiency in successive generations of Ku86$^{-/-}$ mice due to severe infertility of the colony.

## Normal telomeric G-strand overhangs in Ku86$^{-/-}$ cells

To study the telomeric G-strand overhangs of Ku86$^{-/-}$ cells, we carried out TRF analysis with a $(CCCTAA)_4$ probe exactly as described previously (Hemann and Greider, 1999) using non-denaturing pulse-field agarose gels. Detection of a signal with the $(CCCTAA)_4$ probe hybridized to native DNA samples indicates the presence of the G-strand overhang. Figure 5 shows that fresh BM cells from two different Ku86$^{-/-}$ mice showed G-strand specific signals that were similar in size and intensity to those of the corresponding wild-type BM cells. Treatment with mung bean nuclease, which specifically degrades single-stranded DNA and RNA overhangs, showed that the G-strand signal disappeared in all genotypes upon treatment, indicating that the probe was specifically recognizing the single-stranded telomeric tail (Figure 5). As a control, the same gel was denatured and

**Table III.** Measurement by FLOW-FISH of telomere length in splenocytes and bone marrow cells obtained from male (M) and female (F) littermate wild-type and Ku86$^{-/-}$ mice

| Mice | Litter[a] | Genotype | Spleen | | Bone marrow | |
|---|---|---|---|---|---|---|
| | | | Telomere length[b] | Relative length[c] | Telomere length[b] | Relative length[c] |
| AB25 (M) | 1 | Ku86$^{-/-}$ | 14.8 | 124 | | |
| AB30 (F) | | Ku86$^{-/-}$ | 16.4 | 138 | | |
| AB26 (F) | | Wt | 11.9 | 100 | | |
| AB27 (F) | | Wt | 12.2 | 103 | | |
| AB77 (F) | 2 | Ku86$^{-/-}$ | | | 12.8 | 108 |
| AB80 (F) | | Wt | | | 11.9 | 100 |
| AB82 (M) | 3 | Ku86$^{-/-}$ | 8.24 | 105 | 12.6 | 133 |
| AB86 (F) | | Wt | 7.86 | 100 | 9.44 | 100 |
| AB87 (M) | 4 | Ku86$^{-/-}$ | 13.6 | 130 | 13.0 | 108 |
| AB89 (F) | | Wt | 10.5 | 100 | 12.0 | 100 |
| AB88 (M) | 5 | Ku86$^{-/-}$ | 6.47 | 121 | 8.79 | 103 |
| AB92 (F) | | Wt | 5.35 | 100 | 8.56 | 100 |
| AB100 (M) | 6 | Ku86$^{-/-}$ | 5.10 | 125 | 10.8 | 131 |
| AB101 (M) | | Wt | 4.06 | 100 | 8.22 | 100 |

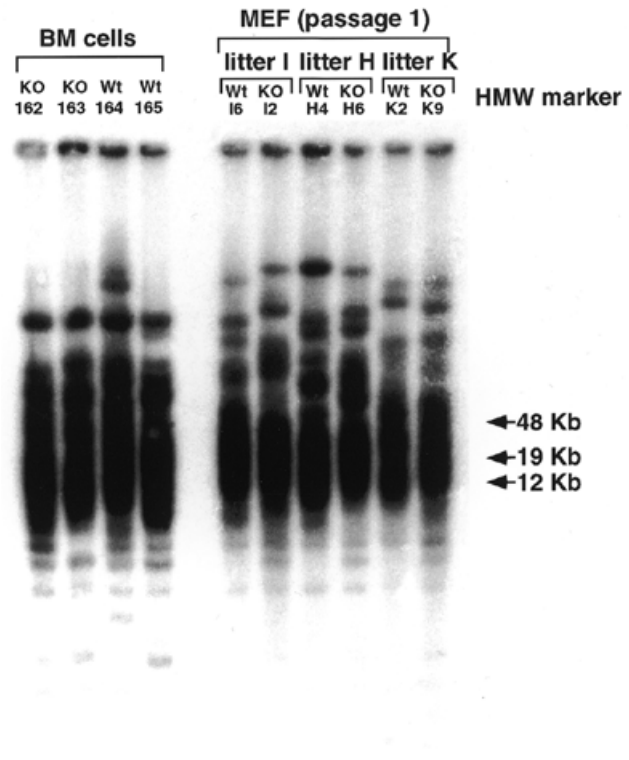


**Fig. 4.** TRF analysis in wild-type and Ku86$^{-/-}$ primary MEFs and BM cells. Three different wild-type (Wt) and Ku86$^{-/-}$ (KO) littermate MEFs (passage 1) were studied, as well as fresh BM samples from two littermate wild-type (Wt) and Ku86$^{-/-}$ (KO) mice. TRF signals were similar in Ku86$^{-/-}$ and wild-type cells. In the case of MEF cultures: I, H and K are three different litters born from heterozygous parents (see also Tables I and II, and Figure 2 for other analyses of the same MEFs). In the case of BM cells, 162, 163, 164 and 165 are mice from the same litter born from heterozygous parents.

rehybridized with the $(CCCTAA)_4$ probe, which highlighted the telomere restriction fragments or TRF (not shown). These results show that Ku86$^{-/-}$ deficiency in mammals does not result in loss or shortening of the G-strand overhang at the telomeres, in contrast to what has been described for yeast Ku proteins (Gravel *et al.*, 1998).

## Ku86 deficiency does not affect telomerase activity

To investigate whether the slightly extended telomeres in Ku86$^{-/-}$ cells can be attributed to a higher telomerase activity in these cells, we quantified telomerase activity in wild-type and Ku86$^{-/-}$ MEFs (passage 1). No significant difference in telomerase activity between wild-type and Ku86$^{-/-}$ littermates was detected (Figure 6). This indicates that Ku86 mutation does not affect telomerase activity, and hence the slightly extended telomeres shown by Ku86$^{-/-}$ cells are not the result of altered telomerase activity in these cells.

# DISCUSSION

Here we describe that Ku86 deficiency in mammals results in a very high frequency of end-to-end fusions relative to other chromosomal aberrations, indicating a function for Ku86 in protecting telomeres from fusions that could be independent from its role in maintaining chromosomal stability (Bailey *et al.*, 1999; Difilippantonio *et al.*, 2000). Furthermore, we show that telomeric fusions triggered by Ku86 deficiency are not mediated by telomere loss nor by deregulation of the telomeric G-strand overhang, in contrast to what has been described in yeast. The impairment of telomere function in Ku86$^{-/-}$-deficient cells is different from that described for the telomerase knock-out mouse (Blasco *et al.*, 1997). Ku86 loss of function is more similar to loss of function of TRF2, a telomere-binding protein that prevents telomere end-to-end fusions in a telomere length-independent manner (van Steensel *et al.*, 1998). However,

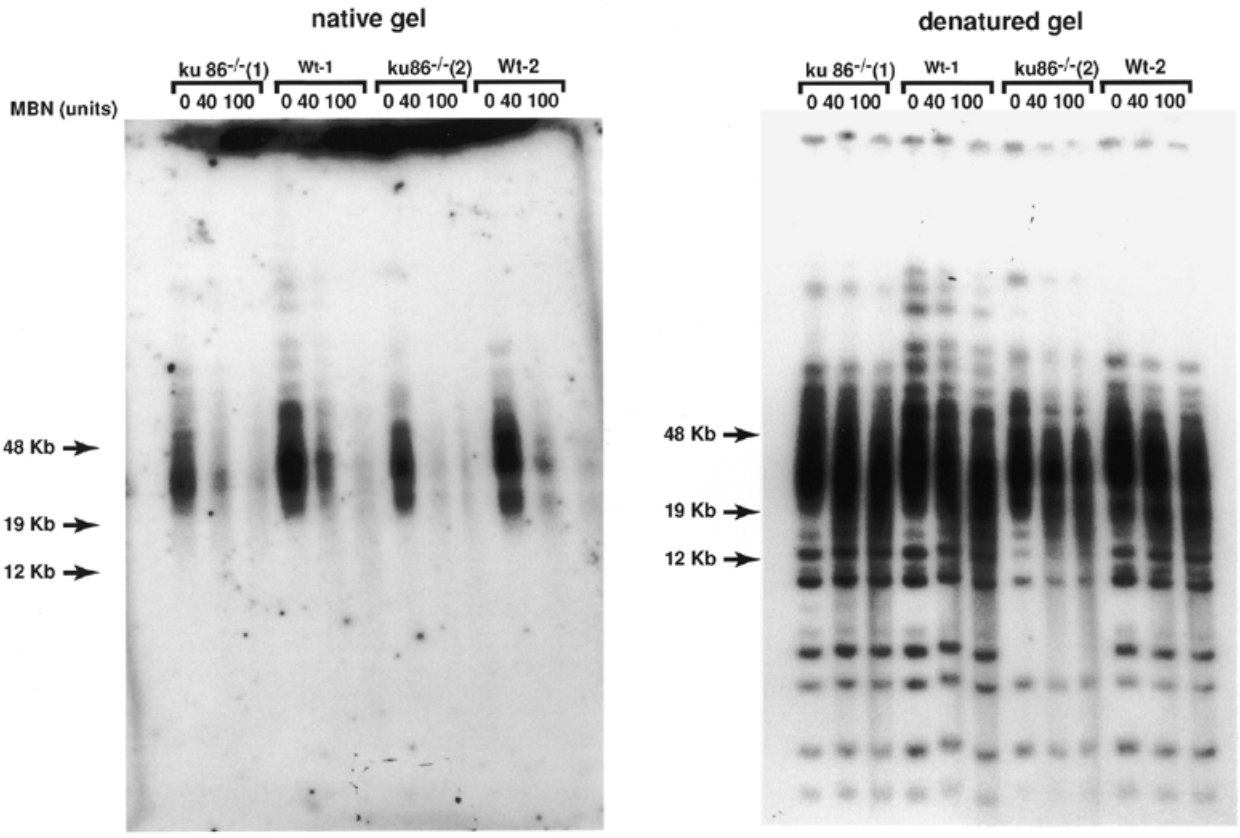


**Fig. 5.** Normal G-strand overhang in Ku86$^{-/-}$ deficient primary cells. G-strand overhangs in fresh BM cells from two littermate wild-type and Ku86$^{-/-}$ mice are visualized in native gel after hybridization with a $(CCCTAA)_4$ probe (see METHODS). Upon treatment with two different doses of mung bean nuclease (MBN), the G-strand specific signal decreases. (1) and (2) are two different litters. As control, the same gel was denatured and reprobed with the $(CCCTAA)_4$ probe to visualize telomeres.

whereas TRF2 loss of function results in shortening of the G-strand overhang at the telomere (van Steensel *et al.*, 1998), Ku86 deficiency does not affect the length of this telomeric structure. This suggests that TRF2 and Ku86 act via independent pathways and that the telomeric fusions occurring in Ku86$^{-/-}$ cells are not likely to be mediated by loss of TRF2 function. It is likely that wild-type Ku86, in combination with other telomeric proteins, prevents the telomere from being recognized as a DSB. Indeed, previous work in yeast suggests that Ku proteins protect the telomeres against recombinases (Polotnianka *et al.*, 1998). The telomere fusions detected in Ku86$^{-/-}$ may represent non-homologous end-joining (NHEJ) events. In this regard, mutations in DNA repair proteins do not necessarily abolish the capability of the cells to carry out NHEJ (Li *et al.*, 1998; DiBiase *et al.*, 2000).

Interestingly, lack of Ku86 results in a moderate telomere lengthening in the absence of changes in telomerase activity levels. This telomere elongation could be the result of a greater accessibility of telomerase and/or homologous recombination proteins to the telomere. Indeed, previous studies of SCID cell lines and SCID mice (impaired for DNA-PKcs function) showed extended telomeres in these cells (Slijepcevic *et al.*, 1997; Hande *et al.*, 1999). The dramatic difference in the effects of Ku86 deficiency in yeast and mammals could be explained, at least in part, by the fact that yeast lacks DNA-PKcs, the partner of Ku proteins in mammals.

Finally, it is tempting to speculate that the roles of Ku86, and possibly of other DNA repair proteins, in aging (Vogel *et al.*, 1999), proliferative capacity of cells (Nussenzweig *et al.*, 1996) and transformation (Difilippantonio *et al.*, 2000) could be mediated by its essential function at the telomere.

## METHODS

**Mice and cells.** The mice used in the study were described by Zhu *et al.* (1996). Wild-type and Ku86$^{-/-}$ mice or cells were derived from heterozygous crosses and, for all studies, littermate wild-type and Ku86$^{-/-}$ mice or cells were used. The age of the mice used for Q-FISH and FLOW-FISH studied ranged from 8 to 12 weeks. MEFs were prepared from day 13.5 embryos derived from heterozygous crosses as described previously (Blasco *et al.*, 1997). First passage MEFs used in the different experiments corresponded to approximately two population doublings (PDL 2).

**Scoring of chromosomal abnormalities.** At least 40 images of each wild-type and Ku86$^{-/-}$ metaphases were scored for telomere fusions, chromatid breaks, chromosome fragments, rings and mini-chromosomes by superimposing the telomere image on the DAPI chromosome image in the TFL-telo

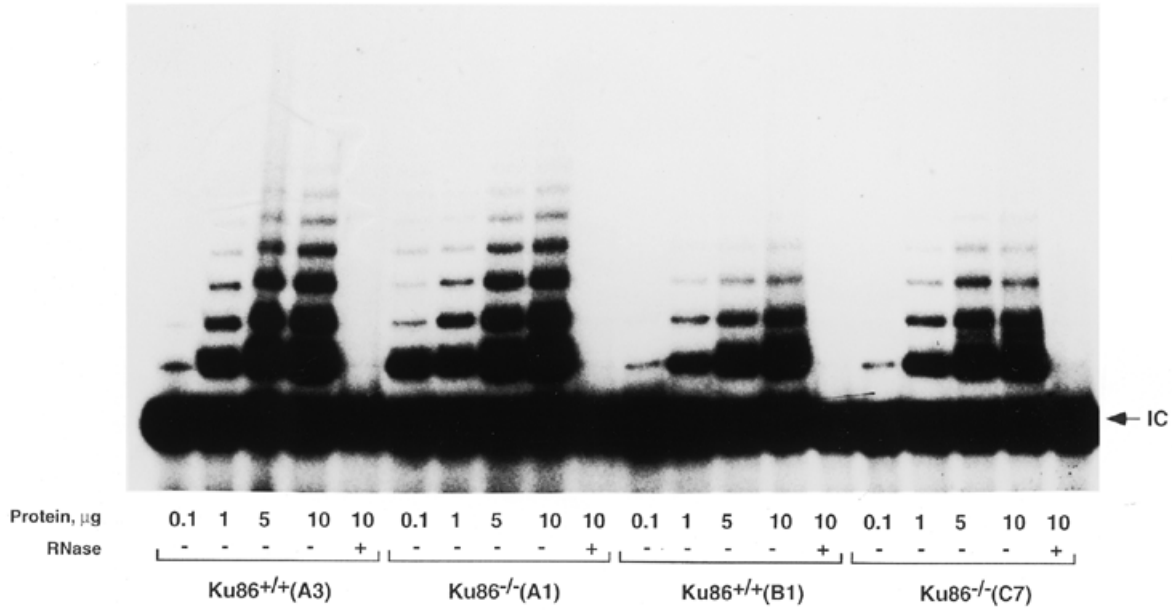


**Fig. 6.** Telomerase activity in wild-type and Ku86$^{-/-}$ MEFs. S-100 extracts were prepared from wild-type (A3 and B1) and Ku86$^{-/-}$ (A1 and C7) MEFs and assayed for telomerase activity. Extracts were pretreated (+) or not (–) with RNase. The protein concentration used is indicated. The arrow indicates the internal control (IC) for PCR efficiency.

programme. The following criteria were applied: telomeric fusions, chromosomes associated by their telomeres with two telomeric signals at the point of fusion; chromatid breaks, gaps in a chromatid whose corresponding chromosome was identified; chromosome fragments, chromosome pieces (with two telomeres or less) whose corresponding chromosome was not easily identified; ring chromosomes, chromosomes with two fused chromatids without a detectable telomeric signal at fusion point; mini-chromosomes, sub-chromosomal fragments with four telomeres.

**Telomere length analysis.** *Q-FISH (Madrid).* First passage MEFs and fresh BM cells were prepared for Q-FISH, and Q-FISH hybridization was carried out as described (Herrera *et al.*, 1999).

To correct for lamp intensity and alignment, images from fluorescent beads (Molecular Probes, USA) were analysed using the TFL-Telo program. Telomere fluorescence values were extrapolated from the telomere fluorescence of LY-R and LY-S lymphoma cell lines (Alexander and Mikulski, 1961) of known lengths of 80 and 10 kb (Samper *et al.*, unpublished results). There was a linear correlation ($r^2$ = 0.999) between the fluorescence intensity of the R and S telomeres with a slope of 38.6. The calibration-corrected telomere fluorescence intensity (ccTFI) was calculated as described (Herrera *et al.*, 1999).

Images were recorded using a COHU CCD camera on a Leica Leitz DMRB fluorescence microscope. A Philips CS 100W-2 Mercury vapor lamp was used as source. Images were captured using Leica Q-FISH software at 400 ms integration time in a linear acquisition mode to prevent over-saturation of fluorescence intensity.

TFL-Telo software (gift from Dr Lansdorp) was used to quantify the fluorescence intensity of telomeres from at least 15 metaphases or fusions of each data point. The images from littermate wild-type and Ku86$^{-/-}$ metaphases were captured on the same day, in parallel, and blindly. All the images from the MEF were captured in a 3 day period after the hybridization.

*Q-FISH (Leiden).* Femurs and testes from 8- to 10-week-old mice were obtained. Air-dried slides were prepared from femur-flushed BM cells and from testes-isolated germ cells using standard cytogenetic techniques. To minimize variability, cells from both wild-type and Ku86$^{-/-}$ mice were dropped on the same slide for each tissue and stored for at least one night at room temperature in air. The staining of slides was as described by De Pauw *et al.* (1998). Only diploid premeiotic stages from testis were analysed.

The instrumentation of digital fluorescence microscopy was as described by Lansdorp *et al.* (1996). Interphase analysis was performed using the algorithm developed by De Pauw *et al.* (1998).

*FLOW-FISH (Madrid).* Fresh BM cells, splenocytes and primary MEFs from littermate wild-type and Ku86$^{-/-}$ animals were prepared as described (Blasco *et al.*, 1997; Herrera *et al.*, 1999). FLOW-FISH hybridization was performed as described (Rufer *et al.*, 1998). To normalize FLOW-FISH data, two mouse leukaemia cell lines (LY-R and LY-S, described above) were used as internal controls in each experiment. The telomere fluorescence of at least 10 000 cells gated at $G_1$–$G_0$ cell cycle stage was measured using a Coulter flow EPICS XL cytometer with the SYSTEM 2 software.

*TRF analysis (Madrid).* Passage 1 MEFs ($5 \times 10^6$) (three wild-type and three littermate Ku86$^{-/-}$) and fresh BM cells (from two wild-type and two Ku86$^{-/-}$ littermate mice) were isolated as described

above and TRF analysis was performed exactly as described in Blasco *et al.* (1997).

**G-strand overhang assay.** The G-strand assay was performed exactly as described (Hemann and Greider, 1999) with minor modifications. Fresh bone marrow cells ($1 \times 10^6$) from two wild-type and two Ku86$^{-/-}$ littermates were included in restriction analysis grade agarose plugs following the manufacturer's instructions (Bio-Rad). After overnight digestion in LDS buffer (1% LDS, 100 mM EDTA pH 8.0, 10 mM Tris pH 8.0), the plugs were digested with either 0, 40 or 100 U mung bean nuclease (MBN) for 30 min. Then the plugs were digested with *Mbo*I overnight and run in a pulse field gel electrophoresis as described previously (Blasco *et al.*, 1997). The sequential in-gel hybridizations in native and denaturing conditions to visualize G-strand overhangs and telomeres, respectively, were carried out exactly as described (Hemann and Greider, 1999).

**Telomerase assay.** S-100 extracts were prepared from wild-type and Ku86$^{-/-}$ primary MEF cultures and a modified version of the TRAP assay was used to measure telomerase activity (Blasco *et al.*, 1996). An internal control for PCR efficiency was included (TRAPeze kit Oncor).

## ACKNOWLEDGEMENTS

We thank E. Santos, E.D. De Paw, A. de Groot and A. van Duijn-Goedhart. We thank M. Serrano for helpful discussions. E.S. and F.G. are supported by the Government of Madrid (CAM). The M.A.B. laboratory is funded by grants PM97-0133 from the Ministry of Science and Technology, Spain, 08.1/0030/98 from CAM, EURATOM/991/0201 and FIGH-CT-1999-00002 from the European Union, and by the Department of Immunology and Oncology of the Centro Nacional de Biotecnología.

## REFERENCES

Alexander, P. and Mikulski, Z.B. (1961) Mouse lymphoma cells with different radiosensitivities. *Nature*, **192**, 572–573.

Autexier, C., and Greider, C.W. (1996) Telomerase and cancer: revisiting the telomere hypothesis. *Trends Biochem. Sci.*, **21**, 387–391.

Bailey, S.M., Meyne, J., Chen, D.J., Kurimasa, A., Li, G.C., Lehnert, B.E. and Goodwin, E.H. (1999) DNA double-strand break repair proteins are required to cap the ends of mammalian chromosomes. *Proc. Natl Acad. Sci. USA*, **96**, 14899–14904.

Bianchi, A. and de Lange, T. (1999) Ku binds telomeric DNA *in vitro*. *J. Biol. Chem.*, **274**, 21223–21227.

Blackburn, E.H. (1991) Structure and function of telomeres. *Nature*, **350**, 569–573.

Blasco, M.A., Rizen, M., Greider, C.W. and Hanahan, D. (1996) Differential regulation of telomerase activity and telomerase RNA during multi-stage tumorigenesis. *Nature Genet.*, **12**, 200–204.

Blasco, M.A., Lee, H.-W., Hande, P., Samper, E., Lansdorp, P., DePinho, R. and Greider, C.W. (1997) Telomere shortening and tumor formation by mouse cells lacking telomerase RNA. *Cell*, **91**, 25–34.

Blasco, M.A., Gasser, S.M. and Lingner, J. (1999) Telomeres and telomerase. *Genes Dev.*, **13**, 2353–2359.

Blunt, T., Gell, D., Fox, M., Taccioli, G.E., Lehmann, A.R., Jackson, S.P. and Jeggo, P.A. (1996) Identification of a non-sense mutation in the carboxyl terminal region of DNA-dependent protein kinase catalytic subunit in the SCID mouse. *Proc. Natl Acad. Sci. USA*, **93**, 10285–10290.

Boulton, S.J. and Jackson, S.P. (1996) Identification of a *Saccharomyces cerevisiae* Ku80 homolog: roles in DNA double strand break rejoining and in telomeric maintenance. *Nucleic Acids Res.*, **24**, 4639–4648.

Boulton, S.J. and Jackson, S.P. (1998) Components of the Ku-dependent non-homologous end-joining pathway are involved in telomeric length maintenance and telomeric silencing. *EMBO J.*, **17**, 1819–1828.

Counter, C.M., Avilion, A.A., LeFeuvre, C.E., Stewart, N.G., Greider, C.W., Harley, C.B. and Bacchetti, S. (1992) Telomere shortening associated with chromosome instability is arrested in immortal cells which express telomerase activity. *EMBO J.*, **11**, 1921–1929.

De Pauw, E.S., Verwoerd, N.P., Duinkerken, N., Willemsze, R., Raap, A.K., Fibbe, W.E. and Tanke, H.J. (1998) Assessment of telomere length in hematopoietic interphase cells using *in situ* hybridization and digital fluorescence microscopy. *Cytometry*, **32**, 163–169.

DiBiase, S.J., Zeng, Z.C., Chen, R., Hyslop, T., Curran, W.J., Jr and Iliakis, G. (2000) DNA-dependent protein kinase stimulates an independently active, nonhomologous, end-joining apparatus. *Cancer Res.*, **60**, 1245–1253.

Difilippantonio, M.J., Zhu, J., Tang-Chen, J., Meffre, E., Nussenzweig, M., Max, E.E., Ried, T. and Nussenzweig, A. (2000) DNA repair protein Ku80 suppresses chromosomal aberrations and malignant transformation. *Nature*, **404**, 510–514.

Gao, Y., Chaudhuri, J., Zhu, C., Davidson, L., Weaver, D.T. and Alt, F.W. (1998) A targeted DNA-PKcs-null mutation reveals DNA-PK-independent functions for Ku in V(D)J recombination. *Immunity*, **9**, 367–376.

Gravel, S., Larrivee, M., Labrecque, P. and Wellinger, R.J. (1998) Yeast Ku as a regulator of chromosomal DNA end structure. *Science*, **280**, 741–744.

Gu, Y.S., Jin, S.F., Gao, Y.J., Weaver, D.T. and Alt, F.W. (1997) Ku70 deficient embryonic stem cells have increased ionizing radiosensitivity, defective DNA end binding activity, and inability to support V(D)J recombination. *Proc. Natl Acad. Sci. USA*, **94**, 8076–8081.

Hande, P., Slijepcevic, P., Silver, A., Bouffler, S., van Buul, P., Bryant, P. and Lansdorp, P. (1999) Elongated telomeres in scid mice. *Genomics*, **56**, 221–223.

Hemann, M.T. and Greider, C.W. (1999) G-strand overhangs on telomeres in telomerase deficient mouse cells. *Nucleic Acids Res.*, **27**, 3964–3969.

Herrera, E., Samper, E., Martín-Caballero, J., Flores, J.M., Lee, H.-W. and Blasco, M.A. (1999) Disease states associated to telomerase deficiency appear earlier in mice with short telomeres. *EMBO J.*, **18**, 2950–2960.

Hsu, H.-L., Gilley, D., Backburn, E. and Chen, D.J. (1999) Ku is associated with the telomere in mammals. *Proc. Natl Acad. Sci. USA*, **96**, 12454–12458.

Lansdorp, P.M., Verwoerd, N.P., van de Rijke, F.M., Dragowska, V., Little, M.-T., Dirks, R.W., Raap, A.K. and Tanke, H.J. (1996) Heterogeneity in telomere length of human chromosomes. *Hum. Mol. Genet.*, **5**, 685–691.

Laroche, T., Martin, S.G., Gotta, M., Gorham, H.C., Pryde, F.E., Louis, E.J. and Gasser, S.M. (1998) Mutation of yeast Ku genes disrupts the subnuclear organization of telomeres. *Curr. Biol.*, **8**, 653–656.

Li, G.C., Ouyang, H.H., Li, X.L., Nagasawa, H., Little, J.B., Chen, D.J., Ling, C.C., Fuks, Z. and Cordón-Cardó, C. (1998) ku70: A candidate tumor suppressor gene for murine T cell lymphoma. *Mol. Cell*, **2**, 1–8.

Martin, S.G., Laroche, T., Suka, N., Grunstein, M. and Gasser, S.M. (1999) Relocalization of telomeric Ku and SIR proteins in response to DNA double-strand breaks. *Cell*, **97**, 621–633.

Mills, K.D., Sinclair, D.A. and Guarente, L. (1999) MEC1-dependent redistribution of the Sir3 silencing protein from telomeres to DNA double-strand breaks. *Cell*, **97**, 609–620.

Nugent, C.I., Bosco, G., Ross, L.O., Evans, S.K., Salinger, A.P., Moore, J.K., Haber, J.E. and Lundblad, V. (1998) Telomere maintenance is dependent on activities required for end repair of double-strand breaks. *Curr. Biol.*, **8**, 657–660.

Nussenzweig, A., Chen, C.H., Soares, V.D., Sanchez, M., Sokol, M.C., Nussenzweig, M.C. and Li, G.C. (1996) Requirement for Ku80 in growth and immunoglobulin V(D)J recombination. *Nature*, **382**, 551–555.

Ouyang, H. *et al.* (1997) Ku70 is required for DNA repair but not for T cell antigen receptor gene recombination *in vivo*. *J. Exp. Med.*, **186**, 921–929.

Polotnianka, R.M., Li, J. and Lustig, A.J. (1998) The yeast Ku heterodimer is essential for protection of the telomere against nucleolytic and recombinational activities. *Curr. Biol.*, **8**, 831–834.

Rufer, N., Dragowska, W., Thornbury, G., Roosnek, E. and Lansdorp, P.M. (1998) Telomere length dynamics in human lymphocyte subpopulations measured by flow cytometry. *Nature Biotechnol.*, **16**, 743–747.

Slijepcevic, P., Hande, M.P., Bouffer, S., Lansdorp, P. and Bryant, P.E. (1997) Telomere length, chromatin structure and chromosome fusigenic potential. *Chromosoma*, **106**, 413–421.

Smith, G.C.M. and Jackson, S.P. (1999) The DNA-dependent protein Kinase. *Genes Dev.*, **13**, 916–934.

van Steensel, B., Smogorzewska, A. and de Lange, T. (1998) TRF2 protects human telomeres from end-to-end fusions. *Cell*, **92**, 401–413.

Vogel, H., Lim, D.-S., Karsenty, G., Finegold, M. and Hasty, P. (1999) Deletion of Ku86 causes early onset of senescence in mice. *Proc. Natl Acad. Sci. USA*, **96**, 10770–10775.

Zhu, C.M., Bogue, M.A., Lim, D.S., Hasty, P. and Roth, D.B. (1996) Ku86-deficient mice exhibit severe combined immunodeficiency and defective processing of V(D)J recombination intermediates. *Cell*, **86**, 379–389.

Zijlmans, J.M., Martens, U.M., Poon, S., Raap, A.K., Tanke, H.J., Ward, R.K. and Lansdorp, P.M. (1997) Telomeres in the mouse have large inter-chromosomal variations in the number of $T_2AG_3$ repeats. *Proc. Natl Acad. Sci. USA*, **94**, 7423–7428.

DOI: 10.1093/embo-reports/kvd051